Force and fabric states in granular media

Farhang Radjai

Force and fabric states in granular media

Farhang Radjai

LMGC, CNRS-Université Montpellier 2, 34095 Montpellier cedex 05, France

Abstract. The plastic flow of granular materials reflects to a large extent the constraints imposed by steric exclusions and mechanical equilibrium at the particle scale. An accurate formulation of these local constraints is the key to a statistical mechanical approach but requires a rich set of state parameters. We show that the constraints can be taken into account in a simple way with a reduced set of anisotropy parameters akin to the lowest-order description of the contact and force networks. We then introduce a model of kinematic jamming defined as a state of saturation in the evolution of the contact network. This model correctly predicts the accessible geometrical states as well as the evolution of the system to a kinematically jammed state. We also show that a harmonic decomposition of shear stress as a function of the anisotropy parameters and phase factors representing the loading history leads to the "fragile" character of force networks.

Keywords: granular materials, plastic behavior, steric exclusions, force network, state parameter, jamming, fragile behavior
PACS: 45.70.-n, 45.50.-j, 61.43.-j, 83.80.Fg

INTRODUCTION

The microstructure is at the focus of much of the current research on granular media, and it has been investigated during the last three decades both by experiments and by discrete element simulations. Not only many scientific issues raised by the granular microstructure are interesting in their own right, but it is also obvious that a fundamental approach based on the microstructure is a necessary step in searching for innovative solutions to industrial challenges. Two parallel viewpoints coexist presently in this field: 1) a materials approach regarding the broad interest and scope of granular materials and 2) a physical approach considering granular media as a metaphor of driven dissipative systems. At the junction of these two routes, we may consider a common denominator pertaining to the granular microstructure, on the one hand, and the variants depending on the particle interactions and particle shape and size distribution, of vital importance to applications, on the other hand.

In this paper, we apply such a methodology basically in the case of plastic deformations of a granular material at low strain rates. The plasticity theory provides a unifying framework for a physical approach based on the microstructure. Two constraints make the behavior depend on nontrivial features of the microstructure: 1) the steric hindrances among neighboring particles, which constrain the accessible geometrical states, and 2) the condition of mechanical equilibrium, which controls to some extent the range of admissible particle configurations [1]. A complete set of internal state parameters allowing for these constraints to be expressed involves multicontact probability density functions that are too rich to be accessed experimentally or tackled theoretically. The issue therefore is to work with the lowest-order description of the microstructure at the price of accounting in a less strict sense for the local constraints [2, 3].

Granular materials have inspired a number of insightful concepts and analogies, that have extended the scope of this field beyond its traditional frontiers. But, to benefit from this expansion of the field, we often need to adapt and define such general concepts on a quantitative basis. A well-known concept is *jamming* defined as the arrest of dynamics in a metastable state [4, 5]. In this paper we show that the concept of jamming can be more naturally associated with the evolution of the contact network, a fundamental aspect of plasticity.

In a similar vein, the concept of "fragile" behavior was defined as the resistance of a material only to a set of compatible stresses, basically those applied during its past deformations [6]. However, such compatible stresses have not been given a precise definition for dense volume-free granular materials. We show that the fragile property can be "demonstrated" within a plausible approximation of the shear stress in terms of fabric and force anisotropies. This again provides a connection with the plasticity theory as far as the yield surface is concerned.

GRANULAR PLASTICITY

We consider slowly sheared granular materials in which the impulsive forces (induced by collisions and unstable particle rearrangements) can be neglected compared to the static forces (induced by a confining pressure). For a confining pressure p (counted positive for compressive stresses) and particles of average diameter d, the contact forces of static origin are of the order of $f_s = pd^2$ in 3D ($f_s = pd$ in 2D). At the same time, for a shear strain

rate $\dot{\varepsilon}_q$, the time scale of the flow is $\Delta t = \dot{\varepsilon}_q^{-1}$ and thus the order of magnitude of the impulsive forces is given by the momentum per unit time $f_i = md\dot{\varepsilon}_q/\Delta t$, where m is the average particle mass. In the quasi-static limit, the condition $f_s \gg f_i$ implies $I \equiv \dot{\varepsilon}_q\sqrt{m/(pd)} \ll 1$ ($I \equiv \dot{\varepsilon}_q\sqrt{m/p}$ in 2D). The inertial number I controls in this way the transition from plastic to visco-plastic flow [7].

In the plastic regime, the behavior is rate-independent and the physical time t can be replaced by a cumulative shear strain ε_q or $\dot{\varepsilon}_q t$ for a constant driving shear rate $\dot{\varepsilon}_q$. As a result, the plastic strain tensor ε_{ij} reflects simply the relative particle displacements, all scaling with ε_q. In particular, using the language of plasticity, the flow rule should be specified by a ratio $\varepsilon_p/\varepsilon_q$ where $\varepsilon_p \equiv \mathrm{tr}(\varepsilon)$ is the volumetric strain. This ratio is often characterized by an angle ψ, the *dilatancy angle*, which defines the direction of the plastic strain rate.

Neglecting impulsive forces in the plastic regime implies that the deformation is a continuous transition between mechanically equilibrated and stable states. The Coulomb friction law and the assumption of perfectly rigid particles, as a physically plausible approximation when the particle stiffness E is small compared to p, involve no characteristic force. Therefore, all contact forces $\vec{f}$ and the stress tensor σ_{ij} must scale with p. In particular, the plastic threshold is characterized by a stress ratio q/p, where q is the stress deviator. This means that the admissible stresses are inside a cone in the stress space. This cone is nothing but the Coulomb cone described by the *internal angle of friction* φ.

The stress and strain invariants (p,q) and $(\dot{\varepsilon}_p,\dot{\varepsilon}_q)$, respectively, are conjugate variables with respect to the total power $\dot{W}$ of the applied stresses. In 3D with axial symmetry and principal strain rates $\dot{\varepsilon}_1$ and $\dot{\varepsilon}_2 = \dot{\varepsilon}_3$, we have $\dot{\varepsilon}_q = \dot{\varepsilon}_1 - \dot{\varepsilon}_2$ and $\dot{\varepsilon}_p = \dot{\varepsilon}_1 + 2\dot{\varepsilon}_2$. In the same way, the principal stresses are σ_1 and $\sigma_2 = \sigma_3$, and we have $q = (\sigma_1 - \sigma_2)/3$ and $p = (\sigma_1 + 2\sigma_2)/3$. The total power is given by $\dot{W} = \sigma_1\dot{\varepsilon}_1 + \sigma_2\dot{\varepsilon}_2 + \sigma_3\dot{\varepsilon}_3 = p\dot{\varepsilon}_p + 2q\dot{\varepsilon}_q$. With these notations, the internal angle of friction and dilatancy angle are defined by $\sin\varphi = 3q/(2p+q)$ and $\sin\psi = 3\dot{\varepsilon}_p/(\dot{\varepsilon}_p - 2\dot{\varepsilon}_q)$, respectively. Notice that ψ is positive for dilation (counted negative for granular materials). Since work is supplied to deform the system, we have $\dot{W} > 0$, and this implies $\varphi > \psi$. Remark that "associated" plasticity would imply $\varphi = \psi$, which is not in agreement with observations. In 2D, we set $\dot{\varepsilon}_q = \dot{\varepsilon}_1 - \dot{\varepsilon}_2$, $\dot{\varepsilon}_p = \dot{\varepsilon}_1 + \dot{\varepsilon}_2$, $q = (\sigma_1 - \sigma_2)/2$ and $p = (\sigma_1 + \sigma_2)/2$, and the angles are given by $\sin\varphi = q/p$ and $\sin\psi = -\dot{\varepsilon}_p/\dot{\varepsilon}_q$.

In the classical soil mechanics approach, the angles φ and ψ are associated with particular states of a granular material subjected to shearing. Two states are of special interest: 1) stress peak and 2) "critical state" that corresponds to a steady flow with no volume change so that $\psi = 0$. But the angles φ and ψ can be defined at *arbitrary* state in the evolution of the material since for their definition we did not refer to the state of the material. Therefore, the granular plasticity is characterized by the state-dependent angles φ and ψ, and the plastic behavior cannot be fully described unless a set of *internal state parameters* is introduced.

It is obvious that in a fundamental approach the internal state parameters should describe the granular microstructure, and are thus of geometrical nature. We refer to such descriptors of the microstructure as *fabric* state parameters. The level of description depends on the choice of these parameters, which should naturally comply with both the accuracy and tractability of the formulation and which can be scalar or tensorial parameters or functions. Let $\mathscr{F}$ represent such a set of fabric parameters. Then, a model of granular plasticity is fully defined by specifying [8, 1]:

1. $\varphi(\mathscr{F})$: the internal angle of friction as a function of the state parameters (yield function);
2. $\psi(\mathscr{F})$: the dilatancy angle as a function of the state parameters (flow rule);
3. $\delta\mathscr{F}(\delta\varepsilon_q)$: the incremental evolution of state parameters with driving strain $\delta\varepsilon_q$ (hardening rule).

In this model, the steady state is characterized by a fabric $\mathscr{F}^*$ for which $\delta\mathscr{F}(\delta\varepsilon_q) = 0$ and $\psi(\mathscr{F}^*) = 0$. The angle of friction $\varphi^* = \varphi(\mathscr{F}^*)$ is the steady-state (or critical-state) angle of friction, a property of the material.

LOCAL CONSTRAINTS

The internal state variables must be rich enough to represent microscopic mechanisms that underlie plastic behavior. Two constraints are generic to all kind of granular material in a quasi-static state and may therefore be regarded as the most basic requirements in a theoretical approach: steric exclusions and mechanical equilibrium. These constraints both have a local character and can be formulated in terms of particle environments.

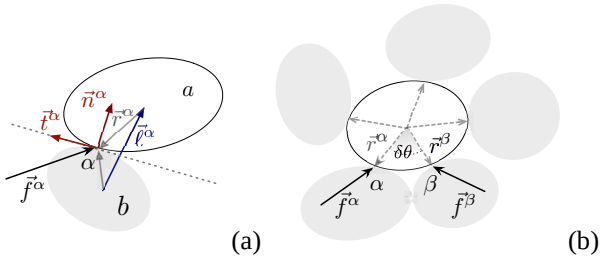

FIGURE 1. (a) The contact geometry; (b) First-shell particle environment with angular exclusions.

In Fig. 1(a) a representation of the contact geometry between a particle a and its contact neighbor b is shown. The relevant geometrical variables are the *contact vector*

$\vec{r} = r\vec{n}$ joining the particle center to the contact point, the *branch vector* $\vec{\ell}$ joining the centers of two contacting particles and the contact orientation vector (contact normal) $\vec{n}'$ defined as the unit vector normal to the particle boundary at the contact zone α. The reaction forces $\vec{f}$ and $-\vec{f}$ acting on the two particles at their contact zone have a unique application point that may be considered as their contact point. We define a local frame composed of the "radial" unit vector $\vec{n}$ and one orthogonal unit vector $\vec{t}$ in an orthoradial plane (orthogonal to the contact vector). In 2D, the local frame is uniquely defined by a single tangent unit vector $\vec{t}$.

We need a statistical description due to granular disorder, with the basic feature that the local vectors vary discontinuously from one contact to another. The local environments fluctuate in space both in the number k of the contacts of each particle (topological disorder) and in their angular positions $\vec{r}^{\alpha}$ (metric disorder). For the formulation of the local constraints only the first contact neighbors of a particle are sufficient. Two functions are required to describe this *first shell* environment [1, 3]:

1. $P_c(k)$: *Connectivity function* defined as the proportion of particles with exactly k contacts (first shells with k members).
2. $P_{kkrf}(\vec{r}^1,\ldots,\vec{r}^k,\vec{f}^1,\ldots,\vec{f}^k)$: *Multicontact probability density function* of k contact forces $\vec{f}^{\alpha}$ and k angular positions $\vec{r}^{\alpha}$ for a shell of k particles.

The average connectivity of the contact network is the coordination number $z = \sum_{k=1}^{\infty} kP_c(k)$. Integration of P_{kkrf} over all angular positions yields the multicontact force pdf's $P_{kkf}(\vec{f}^1,\ldots,\vec{f}^k) = \int_{\mathscr{A}_{kr}} P_{kkrf}\ d\{\vec{r}^{\alpha}\}$, where $\mathscr{A}_{kr}$ is the accessible domain of angular positions. In the same way, the multicontact pdf of angular positions is $P_{kkr}(\vec{r}^1,\ldots,\vec{r}^k) = \int_{\mathscr{A}_{kf}} P_{kkrf}\ d\{\vec{f}^{\alpha}\}$, where $\mathscr{A}_{kf}$ is the integration domain.

In the particle shells, the steric constrains manifest themselves as *angular exclusions*. Two particles belonging to a shell cannot approach one another below a minimum angular interval $\delta\theta_{min}$; see Fig. 1(b). In other words, the multicontact pdf P_{kkr} vanishes if the angular exclusions are violated:

$$P_{kkr}(\vec{r}^1,\ldots,\vec{r}^k) = 0 \quad \text{if} \quad \vec{n}^{\alpha}\cdot\vec{n}^{\beta} > \cos(\delta\theta_{min}) \quad \forall\alpha\neq\beta \tag{1}$$

The exclusion angle $\delta\theta_{min}$ is $\pi/3$ in a monodisperse packing of spheres or disks.

The mechanical equilibrium condition can be expressed as complementarity relations in terms of the multicontact force pdf's:

$$\left(\sum_{\alpha=1}^{k}\vec{f}^{\alpha}\right)P_{kkf} = 0 \ \text{ and } \ \left(\sum_{\alpha=1}^{k}\vec{r}^{\alpha}\times\vec{f}^{\alpha}\right)P_{kkf} = 0 \tag{2}$$

The functions P_c and P_{kkrf} contain a rich amount of information about the the state of a granular system in terms of the fabric and force distributions condensed in the particle environments, and they evolve with the driving strain while keeping to satisfy the constraints. It should, however, be remarked that part of this information is highly redundant. In particular, the functions P_{kkr} and P_{kkf} are strongly correlated since for a mean stress state σ the contact forces can be partially determined for the specified contact network by means of the force and moment balance conditions up to some degree of indeterminacy resulting from the assumption of perfect particle rigidity and Coulomb friction law. However, the contact forces reflect subtle features of the granular microstructure that are more evident to observe through the force network. The surprising inhomogeneity of the force chains could hardly be guessed just from the appearance of the contact network. The inclusion of the forces in the state is therefore a genuine choice in view of taking advantage of the well-known properties of the force network. Owing to their connection with the microstructure, the forces represent the state of the microstructure and, in the last analysis, they can be considered as fabric parameters.

STATE PARAMETERS

The information contained in the local distributions P_c and P_{kkrf} can be reduced in three steps. In the first step, we extract the 1-contact distributions for the shells of k contacts by integration over all contacts except one:

$$\begin{aligned} P_{krf}(\vec{r},\vec{f}) \;=\; & \int_{\mathscr{A}_{kr}}\int_{\mathscr{A}_{kf}} P_{kkrf}(\vec{r}^1,\ldots,\vec{r}^k,\vec{f}^1,\ldots,\vec{f}^k) \\ & \delta(\vec{r}-\vec{r}^1)\,\delta(\vec{r}-\vec{r}^1)d\{\vec{r}^{\alpha}\}d\{\vec{f}^{\alpha}\} \end{aligned} \tag{3}$$

This function is the pdf of a contact at angular position $\vec{r}$ belonging to a shell of k contacts and carrying a force $\vec{f}$. The pdf's of contact positions and forces are given by

$$P_{kr}(\vec{r}) \;=\; \int_{\mathscr{A}_{kf}} P_{krf}\ d\vec{f} \tag{4}$$

$$P_{kf}(\vec{f}) \;=\; \int_{\mathscr{A}_{kr}} P_{krf}\ d\vec{r} \tag{5}$$

where $\mathscr{A}_{kr}$ and $\mathscr{A}_{kf}$ are single-contact integration domains of positions and forces, respectively.

In the second step, we average over the shells by weighting the above 1-contact distributions by P_c:

$$P_{rf}(\vec{r},\vec{f}) \;=\; \sum_{k=1}^{\infty} P_c(k)\,P_{krf}(\vec{r},\vec{f}) \tag{6}$$

$$P_r(\vec{r}) \;=\; \sum_{k=1}^{\infty} P_c(k)\,P_{kr}(\vec{r}) \tag{7}$$

$$P_f(\vec{r}) \;=\; \sum_{k=1}^{\infty} P_c(k)\, P_{kf}(\vec{f}) \qquad (8)$$

These pdf's contain no information about the shells and topological disorder of the contact network and, in contrast to P_{kkrf} and P_{krf}, are π-periodic. We also note that owing to angular exclusions (1) the multicontact pdf P_{kkr} of the angular positions cannot be reduced to a product of the 1-contact pdf's $P_{kr}(\vec{r})$:

$$P_{kkr}(\vec{r}^{\,1},\ldots,\vec{r}^{\,k}) \neq P_r(\vec{r}^{\,1})\cdots P_r(\vec{r}^{\,k}) \qquad (9)$$

Several macroscopic observables are the first moments of the force and fabric distributions. In particular, the average *internal moment tensor* M is given by [9, 10]

$$M = \langle -\vec{r}\otimes\vec{f}\rangle = \int_{\mathscr{A}_r}\int_{\mathscr{A}_f} -\vec{r}\otimes\vec{f}\; P_{rf}(\vec{r},\vec{f})\; d\vec{r}\,d\vec{f} \qquad (10)$$

where $\otimes$ denotes a dyadic product, i.e. $(\vec{r}\otimes\vec{f})_{ij} = r_i f_j$. It can be shown that the average stress tensor σ is simply

$$\sigma = n_p\, M \qquad (11)$$

where n_p is the particle number density. The average pressure is given by $p = \mathrm{tr}(\sigma)/D = -n_p\langle\vec{r}\cdot\vec{f}\rangle/D$.

In discrete writing of (10), each contact α occurs two times in the summation for the two contacting particles a and b with the contribution $r_i^{\alpha a} f_j^{ba} + r_i^{\alpha b} f_j^{ab}$ where $\vec{f}^{ba}$ is the force exerted at the contact point α on particle b by particle a and, conversely, $\vec{f}^{ab}$ is the force exerted at the same contact on particle a by particle b. Since $\vec{f}^{ab} \equiv \vec{f}^{\alpha} = -\vec{f}^{ba}$, the contribution of the contact α to the sum is given by $f_i^{\alpha}\ell_j^{\alpha}$ where $\vec{\ell}^{\alpha} = \vec{r}^{\alpha b} - \vec{r}^{\alpha a}$ is the branch vector. In this way, the stress tensor can be expressed as [11, 12, 13]

$$\sigma = n_c\,\langle\vec{\ell}\otimes\vec{f}\rangle \qquad (12)$$

and in its integral form the pdf $P_{\ell f}(\vec{\ell},\vec{f})$ replaces $P_{rf}(\vec{r},\vec{f})$. We can also define fabric tensors of increasing order from the distribution of contact vectors.

The third step in reducing the information contained in local distributions consists in extracting the angular behavior from $P_{krf}(\vec{r},\vec{f})$. As we shall see below, this angular information determines the deviatoric content of the stress tensor. We consider the force components in the local frame: $\vec{f} = f_n\,\vec{n} + f_t\,\vec{t}$ and define the functions $P_k(\vec{n})$, $\langle f_n\rangle_k(\vec{n})$, $\langle f_t\rangle_k(\vec{n})$ and $\langle r\rangle_k(\vec{n})$ that express explicitly the contact direction dependence of the vectors $\vec{r}$ and $\vec{f}$:

$$\begin{aligned}
P_k(\vec{n}) &= \int_{r=0}^{\infty}\int_{\mathscr{A}_f} P_{krf}(\vec{r},\vec{f})\,dr\,d\vec{f}\\
\langle r\rangle_k(\vec{n})P_k(\vec{n}) &= \int_{\mathscr{A}_f} r P_{krf}(\vec{r},\vec{f})\;d\vec{f}\\
\langle f_n\rangle_k(\vec{n})P_k(\vec{n}) &= \int_{r=0}^{\infty}\int_{\mathscr{A}_f} f_n P_{krf}(\vec{r},\vec{f})\,dr\,d\vec{f}\\
\langle f_t\rangle_k(\vec{n})P_k(\vec{n}) &= \int_{r=0}^{\infty}\int_{\mathscr{A}_f} f_t P_{krf}(\vec{r},\vec{f})\,dr\,d\vec{f}
\end{aligned} \qquad (13)$$

where $\langle\ldots\rangle_k$ denotes averaging at constant values of k and $\vec{n}$. These functions can be averaged over the shells: $P(\vec{n}) = \sum_{k=1}^{\infty} P_k(\vec{n})P_c(k)$, $\langle r\rangle(\vec{n}) = \sum_{k=1}^{\infty}\langle r\rangle_k(\vec{n})P_c(k)$, $\langle f_n\rangle(\vec{n}) = \sum_{k=1}^{\infty}\langle f_n\rangle_k(\vec{n})P_c(k)$ and $\langle f_t\rangle(\vec{n}) = \sum_{k=1}^{\infty}\langle f_t\rangle_k(\vec{n})P_c(k)$.

Figure 2 shows a polar representation of the k-averaged functions for two samples of polyhedra and spheres sheared by triaxial compression by means of contact dynamics simulations. The angular average of branch-vector lengths $\langle\ell\rangle(\vec{n})$ has been shown instead of $\langle r\rangle(\vec{n})$, but the behaviors are similar. The general state of a packing depends on its past history, but shearing has the effect of structuring the packing in a well-defined state, the critical state, where the distributions are unimodal. Such distributions may thus be approximated by low-order terms of spherical harmonics in 3D or Fourier series in 2D.

To avoid unnecessary complication, let us consider axial symmetry about the axis of compression. Then, the function $P(\vec{n})$, where $\vec{n} \equiv (\theta,\phi)$, is independent of the azimuthal angle ϕ. There are nine second-order basis functions $Y_m^l(\theta,\phi)$. But only the functions compatible with axial symmetry, namely independent with respect to ϕ and π-periodic as a function of the zenith angle θ, are admissible. The only admissible functions are therefore $Y_0^0 = 1$ and $Y_2^0 = 3\cos^2\theta - 1$, and at leading order we have

$$\begin{aligned}
P_k(\theta) &\simeq \tfrac{1}{4\pi}\{1 + a_{kc}[3\cos^2(\theta-\theta_{kc}) - 1]\}\\
\langle r\rangle_k(\theta) &\simeq r_{km}\{1 + a_{kr}[3\cos^2(\theta-\theta_{kc}) - 1]\}\\
\langle f_n\rangle_k(\theta) &\simeq f_{km}\{1 + a_{kn}[3\cos^2(\theta-\theta_{kf}) - 1]\}\\
\langle f_t\rangle_k(\theta) &\simeq f_{km}\, a_{kt}\sin 2(\theta-\theta_{kf})
\end{aligned} \qquad (14)$$

where a_{kc}, a_{kr}, a_{kn} and a_{kt} are the anisotropy parameters of the k-shells, r_{km} is their mean contact vector length, and f_{km} the mean force. The privileged directions of the contact vectors and forces are θ_{kc} and θ_{kf}, respectively. P_k is normalized to 1 ($\int P_k(\theta)\sin\theta\, d\theta\, d\phi = 1$).

The sine function for the expansion of the orthoradial component $\langle f_t\rangle_k(\theta)$ is imposed by the requirement that the mean orthoradial force is zero, satisfying the balance of force moments on the particles ($\int P_k(\theta)\langle f_t\rangle_k(\theta)\sin\theta\, d\theta\, d\phi = 0$). Numerical simulations indicate that θ_{kc} and θ_{kf} are generally independent of k. Moreover, a_{kf} is nearly independent of k whereas a_{kc} is crucially dependent on k, as we shall see below. The anisotropies a_{kr} are negligibly small for spherical particles, but have small values otherwise as observed in Fig. 2 [14]. Similar expansions are obtained in 2D by replacing the function $3\cos^2\theta - 1$ by $\cos 2\theta$ and $1/(4\pi)$ by $1/(2\pi)$. We will refer to the above expansions as a *harmonic approximation* of the granular state in the k-shells.

A similar approximation can be made for the shell-averaged functions [11, 12, 15, 13]. At this level of shell-averaged information, the internal state parameters

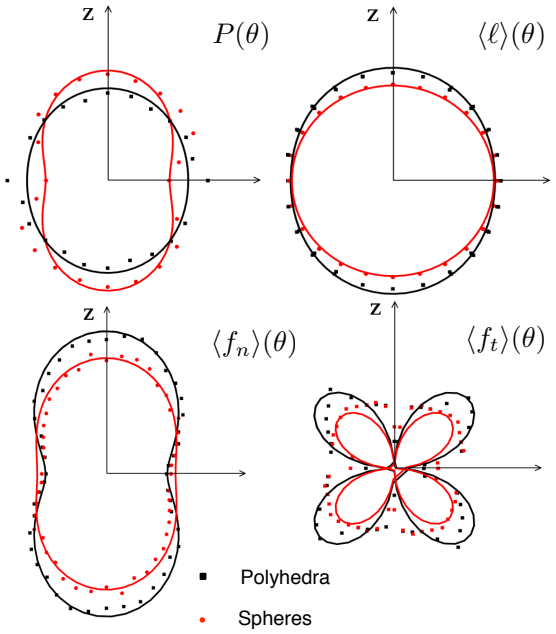

FIGURE 2. Four functions representing the fabric and force states for two packings of spheres and polyhedra triaxially-compressed along the z-axis by means of contact dynamics simulations. The polar angle is the zenith angle in spherical coordinates. The symbols are the simulation data whereas the solid lines are fits by the lowest-order spherical harmonics.

are $z = \sum_k kP_c(k)$, $a_c = \sum_k P_c(k)\, a_{kc}$, $a_r = \sum_k P_c(k)\, a_{kr}$, $a_n = \sum_k P_c(k)\, a_{kn}$ and $a_t = \sum_k P_c(k)\, a_{kt}$, as well as the corresponding phases $\theta_c \simeq \theta_{kc}$ and $\theta_f \simeq \theta_{kf}$ where it is assumed that θ_{kc} and θ_{kf} are independent of k. Therefore, within this global harmonic approximation of the granular state, the plastic behavior is characterized by

1. The evolution of the set of state parameters $\mathscr{F} = \{z, a_c, a_r, a_n, a_t, \theta_c, \theta_f\}$ with the driving strain ε_q
2. The functional dependence of φ and ψ with respect to this set

Some aspects of this problem will be discussed in the following for the simple case of a monodisperse packing of disks.

KINEMATIC JAMMING

As a result of local constraints, the state parameters cannot take arbitrary values. The accessible range of state parameters contains part of the underlying constraints and its knowledge may thus partially replace the higher-order information. For illustration, let us consider the harmonic representation (14) of 1-contact functions. The angular exclusions (1) imply that in a k-shell there can be at most one particle in an angular interval $[-\delta_{min}/2, \delta_{min}/2]$ [3]:

$$\int_{-\frac{\delta_{min}}{2}}^{\frac{\delta_{min}}{2}} kP_k(\theta)\, d\theta \leq 1 \qquad (15)$$

Substituting the harmonic expansion of $P_k(\theta)$ from Eq. (14) in (15) and integrating with respect to θ, we get

$$a_{kc} \leq a_{kc}^{max} = \frac{2\pi}{\sin(\delta\theta_{min})} \left\{ \frac{1}{k} - \frac{1}{z^{max}} \right\} \qquad (16)$$

where $z^{max} = 2\pi/\delta\theta_{min}$. There is therefore an upper bound a_{kc}^{max} depending on k for the shell anisotropies due to steric exclusions. This leads to an upper bound $a_c^{max} = \sum_k P_c(k)\, a_{kc}^{max}$ on the global anisotropy with the approximation that θ_{kc} is independent of k. This example demonstrates clearly the effect of steric exclusions and its scale-up to the macroscopic scale.

The presence of steric exclusions does not prevent granular motion unlike jamming transition where a full arrest of dynamics occurs. But the particle movements are greatly affected when a state of saturation such as a maximum of anisotropy is reached in the course of deformation. We will refer to such states of saturation as *kinematically jammed states*. Below, we propose a simple model that allows us to illustrate this concept and evaluate explicitly the effect of local constraints.

Let us consider a monodisperse packing of disks. We have $a_r = 0$, and the fabric parameters in harmonic approximation are $\{z, a_c, \theta_c\}$. The fabric state can be represented by a single function defined by [1]

$$E(\varepsilon_q, \theta) = \frac{z(\varepsilon_q)}{2\pi} \{1 + a_c(\varepsilon_q) \cos 2[\theta - \theta_c(\varepsilon_q)]\} \qquad (17)$$

Note that $\langle E \rangle_\theta = z$ and $\langle E \cos 2\theta \rangle_\theta = a_c$, where $\langle \cdots \rangle_\theta$ denotes angular averaging.

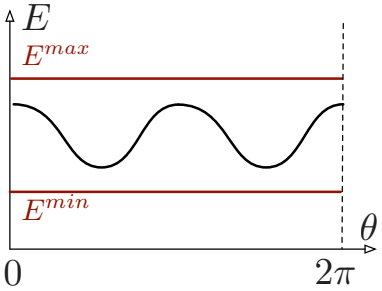

FIGURE 3. Limit states $E^{min}(\theta)$ and $E^{max}(\theta)$, and the general fabric state $E(\theta)$ in the harmonic approximation.

In a co-rotating reference frame with axes oriented along $\theta_c(\varepsilon_q)$ and $\theta_c(\varepsilon_q) + \pi/2$, the fabric state is defined by its position in the space of coordinates z and a_c. The coordination number z is bounded between two limits z^{min} and z^{max}. The upper bound z^{max} is dictated by steric exclusions as discussed before. The lower bound

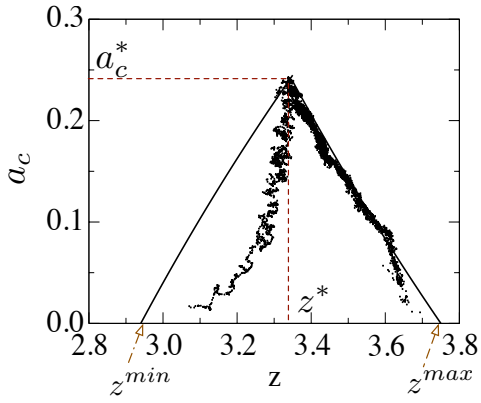

FIGURE 4. Evolution of the fabric state (z, a_c) for a packing of disks biaxially sheared by contact dynamics simulations. The limit states predicted by a model of kinematic jamming (Eq. 18) are shown as well.

z^{min} is related to the condition of mechanical equilibrium. For example, stable particles often involve more than three contacts in 2D and more than four contacts in 3D. To be more precise about these limit mechanical states, we must also specify the value of a_c. We thus define two limit states: 1) the *loosest isotropic state*, characterized by $E^{min}(\theta) = z^{min}/(2\pi)$, and 2) the *densest isotropic state*, characterized by $E^{max}(\theta) = z^{max}/(2\pi)$. These states can be reached only by complex loading. For example, it is generally difficult to bring a granular system towards a dense isotropic state via isotropic compaction. The reason is that the rearrangements occur mainly in the presence of shearing, which leads to fabric anisotropy.

We assume that all accessible fabric states $E(\theta)$ are enclosed between the two isotropic limit states: $E^{min}(\theta) \leq E(\theta) \leq E^{max}(\theta)$; see Fig. 3. This assumption simply means that the same bounds z^{min} and z^{max} govern the limiting number of contacts at each space direction. It is easy to show that this assumption leads to an upper bound on the anisotropy:

$$a_c^{max}(z) = 2\min\left\{1 - \frac{z^{min}}{z}, \frac{z^{max}}{z} - 1\right\} \qquad (18)$$

By construction, $a_c^{max}(z^{min}) = a_c^{max}(z^{max}) = 0$. The largest anisotropy is

$$a_c^\star = a_c^{max}(z^\star) = 2\frac{a_c^{max} - a_c^{min}}{a_c^{max} + a_c^{min}} \qquad (19)$$

with $z^\star = (z^{min} + z^{max})/2$. According to Eq. (19), a_c^{max} increases with z for $z < z^\star$, and it declines with z for $z < z^\star$. In this model, only the states below $a_c^{max}(z)$ are accessible. The points on the frontier of $a_c^{max}(z)$ represent the states with either a saturation of contact gain (to the right of $z^\star$) due to angular exclusions or with a saturation of contact loss (to the left of $z^\star$) due to the condition of mechanical equilibrium. The intersection point $(z^\star, a_c^\star)$ represents the critical state where both contact loss and contact gain are saturated.

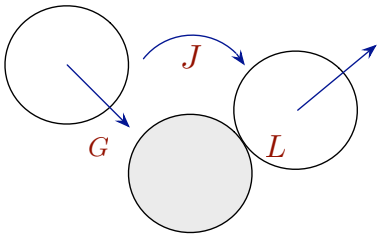

FIGURE 5. The three events of gain (rate G), advection (current J) and loss (rate L) of contacts, governing the evolution of the contact network (fabric state).

Figure 4 shows the evolution of a_c with z in simulated biaxial compression of two initially isotropic samples with coordination numbers $z_0 = 3.1$ and $z_0 = 3.7$. In both simulations, z tends to the same critical-state value $z^\star \simeq 3.35$ with $a_c^\star \simeq 0.24$. Remarkably, the anisotropy of the dense packing reaches and then follows closely the limit states. Eq. (18) provides here an excellent fit to the data with only one fitting parameter z^{max}. In the case of the loose sample, the trajectory remains entirely inside the accessible domain and the boundary is reached only at the critical state. The simulations suggest that the loss saturation limit is difficult to achieve by shearing since in the contact loss regime the anisotropy increases often by contact gain.

Equation (19) predicts that the critical state anisotropy $a_c^\star$ increases with $z^{max} - z^{min}$. The shape, size and frictional characteristics of the particles may therefore influence $a_c^\star$ via z^{min} and z^{max}. For example, increasing the sliding friction coefficient between the particles allows for lower values of z^{min} (stable configurations with less contacts) without changing z^{max} (which depends only on steric exclusions) and leads to larger values of $a_c^\star$.

In exception to the two isotropic limit states, all states of saturation are anisotropic. Hence, the loss and gain saturation occur in particular directions. For this reason the loss and gain of contacts should be considered as a function of space direction θ. Moreover, a number of contacts are advected in the angular space $[0, 2\pi]$ in the sense that the contact normal of an enduring contact rotates. This advection of contacts results in a continuous change of the fabric state $E(\varepsilon_q, \theta)$ whereas the contact loss and gain are discontinuous events. The three elementary "events" of gain, loss and advection of the contacts occur at different rates depending of the space direction: a gain rate $G(\varepsilon_q, \theta)$, a loss rate $L(\varepsilon_q, \theta)$ and a current $J(\varepsilon_q, \theta)$ of advected contacts, respectively. The evolution

of E is governed by a detailed balance equation [8]:

$$\frac{\partial E}{\partial \varepsilon_q} + \frac{\partial J}{\partial \theta} = G - L \tag{20}$$

We expect that G has its largest value along the direction of contraction whereas L is maximal along the direction of extension. The current J is basically given by the number density of contacts times the shear strain in each direction. Hence, the three functions depend actually on the velocity field. In the steady state, we have $\partial J/\partial\theta = G - L$, which means that on average the contacts are gained in the direction of contraction and advected towards the direction of extension where they are lost; see Fig. 5.

Remark that in the absence of J, the relative number E of contacts in each direction would be a simple time accumulation of the contacts induced by loss and gain. During a quasi-static deformation the gain and loss rate functions do not vanish. As long as the system is far from the limit states we may rely on the homogeneous strain field. But the gain and loss rates are modified in the vicinity of the saturation states. In particular, they vanish along θ_c and $\theta_c + \pi/2$, respectively. This feature justifies the description of the states of gain saturation as jammed states whereas the states of loss saturation may be described as "anti-jammed" states! In this respect, the critical state corresponds to a fully jammed state in the statistical sense where both contact gain and loss are saturated although the deformation continues to induce gain and loss of contacts in different directions.

FRAGILE BEHAVIOR

As discussed before, the yield function in a particle-scale approach corresponds to the internal angle of friction φ or the normalized stress deviator q/p as a function of the internal state parameters. This can be achieved with harmonic approximation and the expression (12) of the stress tensor. Indeed, the shell-averaged Fourier expansions of the fabric are

$$\begin{array}{rcl} P(\theta) & \simeq & \frac{1}{2\pi}\{1 + a_c \cos 2(\theta - \theta_c)\} \\ \langle \ell \rangle(\theta) & \simeq & \ell_m \{1 + a_\ell \cos 2(\theta - \theta_c)\} \\ \langle f_n \rangle(\theta) & \simeq & f_m \{1 + a_n \cos 2(\theta - \theta_f)\} \\ \langle f_t \rangle(\theta) & \simeq & f_m \, a_t \sin 2(\theta - \theta_f) \end{array} \tag{21}$$

These functions are involved in the expression of the stress tensor, which in its integral form is given by

$$\sigma_{ij} = n_c \int_{\mathscr{A}_\ell} \int_{\mathscr{A}_f} \ell_i f_j \, P_{\ell f}(\vec{\ell}, \vec{f}) \, d\vec{\ell} \, d\vec{f} \tag{22}$$

Integrating with respect to the forces and considering the definitions (13), averaged over the k-shells, we get [11]

$$\sigma_{ij} = n_c \int_0^{2\pi} \langle \ell \rangle(\theta) P(\theta) \{ \langle f_n \rangle(\theta) \, n_i(\theta) + \langle f_t \rangle(\theta) \, t_j(\theta) \} d\theta \tag{23}$$

Inserting the Fourier expansions (21) in Eq. (23), and integrating with respect to θ, yields the two following interesting relations:

$$p \simeq \frac{1}{2} n_c \ell_m f_m \tag{24}$$

$$\frac{q}{p} \simeq \frac{1}{2}\{(a_c + a_\ell)\cos 2(\theta_\sigma - \theta_c) + (a_n + a_t)\cos 2(\theta_\sigma - \theta_f)\} \tag{25}$$

where θ_σ is the major principal stress direction and the cross products among the anisotropies are neglected. The same relations hold also in 3D under axial symmetry with the factor $1/2$ replaced by $1/3$ in equation (24) and by $2/5$ in equation (25). The two relations (24) and (25) are *state functions* of a granular assembly in the framework of harmonic approximation.

Equation (25) provides a nice fit to the simulation data both in 2D and 3D. It reveals an important property of granular plasticity: The shear strength reflects the ability of a granular system to develop force and fabric anisotropies. This aspect was first demonstrated many years ago by Rothenburg and Bathurst [11]. Except in transients, the fabric and force states are co-axial with the stress state so that $\theta_c = \theta_f = \theta_\sigma$. As a result, we have $q/p \simeq 0.5(a_c + a_\ell + a_n + a_t)$ during a monotonic deformation. The anisotropy a_ℓ of the branch vector lengths can be small but takes non-negligible values for polydisperse systems and non-spherical particles [14, 16]. The relative values of the other anisotropies depend on the composition (shape and particle sizes). It is also important to remark that q/p does not directly depend on z.

Here, we would like to underline another important property of the yield function resulting from the phase differences $\theta_\sigma - \theta_c$ and $\theta_\sigma - \theta_f$ in Eq. (25). Owing to the phase factors, the shear strength q/p depends on the loading direction. For example, when the loading direction θ_σ is reversed (i.e. for a rotation of $\pi/2$ of the applied stress directions), the phase factor $\cos 2(\theta_\sigma - \theta_c)$ changes sign since θ_c (the fabric) doe not react instantly. Therefore, a discontinuous loss of strength occurs during such transients. This property is akin to the *fragile behavior*, which can be formulated by stating that *the largest shear strength of a granular material occurs along the loading path that conducted the system to its present state*. In particular, the shear stress is $q_1/p \simeq 0.5(a_c + a_\ell + a_n + a_t)$ for $\theta_\sigma = \theta_f = \theta_c$ in the critical state and $q_2/p \simeq 0.5(-a_c - a_\ell + a_n + a_t)$ for $\theta_\sigma = \theta_f = \theta_c + \pi/2$. This loss of strength of the order of $a_c + a_\ell$ can be observed in Fig. 6 when the shear strain is reversed.

There is an asymmetry between the response times of contact loss, which is governed by the elastic deformation of the particles, and contact gain, which depends on

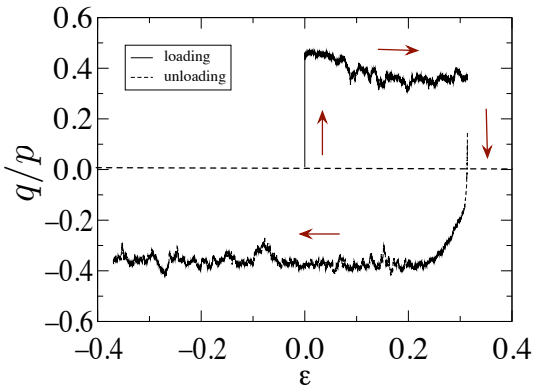

FIGURE 6. Evolution of the shear stress q/p as a function of cumulative shear strain for an initially dense sample, and following shear strain reversal.

the packing geometry (distribution of gaps between the particles). Contact loss is faster than contact gain in a dense packing whereas contact gain prevails in a loose packing. Only in the critical state the loss and gain rates are equal as long as a monotonic shear strain is applied. The response time of contact forces is controlled by particle elasticity and is thus of the same order of magnitude as for contact loss. As a result, upon strain reversal, a fast decrease of shear stress mainly due to the phase difference $\theta_\sigma - \theta_c$ is followed by a long transient where the fabric evolves until the critical state is reached in the new loading direction.

CONCLUSION

In this paper, a particle-scale formulation of granular plasticity was proposed. Two local constraints are essential in this approach: 1) the angular exclusions and 2) the mechanical equilibrium. Multicontact probability density functions are necessary for a full expression of these constraints. But it is possible to work with a lower-order description of the microstructure at the price of accounting in a less strict way for the local constraints. This was shown by a simple model of accessible fabric states in terms of the coordination number and fabric anisotropy by assuming a *harmonic representation* of the force and fabric states. The states of saturation in contact gain and loss were described as *kinematic jamming* and a general formulation of the evolution of the contact network was presented. The shear strength was expressed as a state function involving the fabric and force anisotropies and the stress-fabric and stress-force phase differences. The *fragile behavior* was interpreted as a consequence of the dependence of shear strength on the loading direction.

The specific behavior of each granular material fits to the generic picture presented in this paper. For example, the relative importance of the force and fabric anisotropies depend on the material. The same analysis can also be applied to cohesive granular media where tensile contacts come into play. This framework has also the advantage of bringing together familiar concepts of plasticity, some of the tools and concepts developed in mechanics of granular materials and some recent concepts and ideas put forward in rheology of colloids.

ACKNOWLEDGMENTS

It is a great pleasure to thank Stéphane Roux who originated the idea of granular plasticity with geometrical internal variables.

REFERENCES

1. S. Roux and F. Radjai, "Statistical approach to the mechanical behavior of granular media," in *Mechanics for a New Millennium*, edited by H. Aref, and J. Philips, Kluwer Acad. Pub., Netherlands, 2001, pp. 181–196.
2. F. Radjai, H. Troadec, and S. Roux, "Key features of granular plasticity," in *Granular Materials: Fundamentals and Applications*, edited by S. Antony, W. Hoyle, and Y. Ding, RS.C, Cambridge, 2004, pp. 157–184.
3. H. Troadec, F. Radjai, S. Roux, and J. Charmet, *Phys. Rev. E* **66**, 041305 (2002).
4. A. J. Liu and S. R. Nagel, *Jamming and Rheology*, Taylor and Francis, New York, 2001.
5. A. J. Liu and S. R. Nagel, *Nature* **396**, 21–22 (1998).
6. M. E. Cates, J. P. Wittmer, J.-P. Bouchaud, and P. Claudin, *Phys. Rev. Lett.* **81**, 1841–1844 (1998).
7. GDR-MiDi, *Eur. Phys. J. E* **14**, 341–365 (2004).
8. S. Roux and F. Radjai, "Texture-dependent rigid-plastic behaviour," in *Physics of Dry Granular Media*, edited by H. Herrmann, J. Hovi, and S. Luding, Kluwer Acad. Pub., Dordrecht, 1999, pp. 229–235.
9. J. J. Moreau, "Numerical Investigation of Shear Zones in Granular Materials," in *Friction, Arching, Contact Dynamics*, edited by D. E. Wolf, and P. Grassberger, World Scientific, Singapore, 1997, pp. 233–247.
10. L. Staron, F. Radjai, and J.-P. Vilotte, *Eur. Phys. J. E* **18**, 311–320 (2005).
11. L. Rothenburg and R. J. Bathurst, *Geotechnique* **39**, 601–614 (1989).
12. B. Cambou, "From global to local variables in granular materials," in *Powders and Grains 93*, edited by C. Thornton, A. A. Balkema, Amsterdam, 1993, pp. 73–86.
13. H. Ouadfel and L. Rothenburg, *Mechanics of Materials* **33**, 201–221 (2001).
14. E. Azéma, G. Saussine, and F. Radjai, *Mechanics of Materials* **41** (2009). 41, 729–741 (2009).
15. F. Radjai, D. E. Wolf, M. Jean, and J. Moreau, *Phys. Rev. Lett.* **80**, 61–64 (1998).
16. C. Voivret, F. Radjai, J.-Y. Delenne, and M. S. El Youssoufi, *Phys. Rev. Lett.*, **102**, 178001 (2009).